Biophysical Chemistry 159 (2011) 142–151

Contents lists available at ScienceDirect

Biophysical Chemistry

journal homepage: http://www.elsevier.com/locate/biophyschem

In vivo tests of thermodynamic models of transcription repressor function

Sudheer Tungtur [a], Harlyn Skinner [b], Hongli Zhan [a,1], Liskin Swint-Kruse [a,*], Dorothy Beckett [b,**]

[a] Department of Biochemistry and Molecular Biology, 3901 Rainbow Blvd, University of Kansas Medical Center, Kansas City, KS 66160, United States
[b] Department of Chemistry & Biochemistry, University of Maryland, College Park, MD 20742, United States

ARTICLE INFO

Article history:
Received 31 March 2011
Received in revised form 26 May 2011
Accepted 5 June 2011
Available online 15 June 2011

Keywords:
LacI
GalR
BirA
Repression
Protein-DNA affinity
Equilibrium

ABSTRACT

One emphasis of the Gibbs Conference on Biothermodynamics is the value of thermodynamic measurements for understanding behaviors of biological systems. In this study, the correlation between thermodynamic measurements of *in vitro* DNA binding affinity with *in vivo* transcription repression was investigated for two transcription repressors. In the first system, which comprised an engineered LacI/GalR homolog, mutational changes altered the equilibrium constant for binding DNA. Changes correlated with altered repression, but estimates of *in vivo* repressor concentration suggest a ≥25-fold discrepancy with *in vitro* conditions. In the second system, changes in ligand binding to BirA altered dimerization and subsequent DNA occupancy. Again, these changes correlate with altered *in vivo* repression, but comparison with *in vitro* measurements reveals a ~10-fold discrepancy. Further analysis of each system suggests that the observed discrepancies between *in vitro* and *in vivo* results reflect the contributions of additional equilibria to the transcription repression process.

One of the founders of the Gibbs Conference on Biothermodynamics, Gary Ackers stressed the limited value of biothermodynamic measurements that are divorced from biology. Indeed thermodynamic measurements provide the foundation for quantitative predictions of biological function. However, the ability to predict function for complex biological systems requires detailed investigation of a system's constituent interactions. This entails first defining the thermodynamic (and kinetic) rules that govern pairwise interactions between the relevant biomolecules, followed by quantifying the extent of coupling between the interactions. Once established, the rules can be used to construct testable, statistical thermodynamic models of the system's behavior. This manuscript describes initial studies for reconciling *in vitro* and *in vivo* protein-DNA binding for two transcription repression systems.

In transcription regulation, the probability of initiation is directly related to the ability of the RNA polymerase to access promoter sequences. For the promoters of many prokaryotic genes, polymerase binding must compete with binding by repressor proteins with diminished polymerase access repressing transcription of the downstream genes. Thus, the problem of predicting gene expression can be simplified to predicting repressor occupancy of the relevant DNA binding site(s) (usually called "operators"). However, in many systems, repressor occupancy is the outcome of multiple coupled equilibria, which provide mechanisms for environmental, metabolic, and evolutionary control of transcription.

The work in this manuscript addresses the question of whether well-characterized alterations of *in vitro* DNA occupancy can accurately predict changes in repression *in vivo*. Two separate transcription repressors are considered. The first is an engineered LacI/GalR homolog. Mutagenesis is used to vary the K_d for *lacO*[1] DNA, which results in altered *in vivo* repression of the *lac* operon (*lacZYA*). The second system comprises the wild-type BirA transcription repressor, which requires substrate binding and resulting homodimer formation prior to DNA binding. By altering the *in vivo* substrate concentration, operator occupancy (and thus repression) is altered in a predictable way. Although the two systems show good correlation between *in vitro* thermodynamic parameters and *in vivo* repression, systematic offsets between the *in vivo* and *in vitro* datasets are observed. Potential contributions to these offsets include additional coupled equilibria, differences in *in vivo* and *in vitro* solution conditions, and uncertainties associated with intracellular protein concentrations.

1. The LacI/GalR transcription repressors

Homologs in the family of LacI/GalR transcription regulators control many aspects of bacterial metabolism in response to changes in concentrations of small molecule metabolites [1,2]. All of the well characterized homologs – including LacI [3], PurR [4], GalR [5], and CcpA [6] – require homodimer formation (Fig. 1A) in order to achieve high affinity binding to a pseudo-palindromic operator sequence. A

* Corresponding author. Tel.: +1 913 588 0399; fax: +1 913 588 9896.
** Corresponding author. Tel.: +1 301 405 1812; fax: +1 301 314 9121.
E-mail addresses: lswint-kruse@kumc.edu (L. Swint-Kruse), dbeckett@umd.edu (D. Beckett).
[1] Current address: Greenwood Genetic Center, Greenwood, South Carolina.

0301-4622/$ – see front matter © 2011 Elsevier B.V. All rights reserved.
doi:10.1016/j.bpc.2011.06.005

few family members (such as LacI; [7]) form tetramers that can simultaneously bind and bridge two operators, thereby forming a loop [8]. Most LacI/GalR homologs repress transcription. When the repressor protein is bound to the DNA operator by an N-terminal DNA-binding domain, transcription of downstream genes is reduced [1,2].

Several LacI/GalR transcription repressors have been engineered in the Swint-Kruse lab. In this work, the "LLhG" chimeric repressor is utilized to investigate the correlation between changes in DNA binding affinity (K_d) and effects on *in vivo* repression. LLhG comprises the *Escherichia coli* LacI DNA-binding domain and linker region joined to the regulatory domain of *E. coli* GalR [9] (Fig. 1A). Using 10 variants of LLhG, DNA binding affinities have been determined *in vitro* for the $lacO^1$ operator. The $lacO^1$ operator is the primary operator for repressing the *lac* operon *in vivo* (Fig. 1B). If a mutation leads to a change in binding affinity, a change in repression is also expected.

In vivo, repression of the *lac* operon can be affected by at least three other thermodynamic processes. First, the LacI/GalR repressor proteins bind allosteric ligands that alter affinity for the operator (Fig. 1C); LLhG variants bind the GalR ligands galactose and fucose [9]. Second, the *lac* operon contains two secondary operators, $lacO^2$ and $lacO^3$ (Fig. 1D). Simultaneous binding to two of the three operators by the natural, tetrameric LacI repressor, enhances repression up to 50-fold [8,10,11]. Third, the operator binding sites are always in competition with excess *E. coli* genomic DNA for binding to repressor protein [12] (Fig. 1D). For wild-type LacI, nonspecific DNA binding is key for inducing transcription of *lacZYA*; binding of the allosteric ligand to the proteins diminishes the binding affinity for operator by ~1000-fold, at which point excess genomic DNA effectively competes for repressor protein so that the operator is vacated [12,13] (Fig. 1C).

A few prior studies have examined the *in vivo* behavior of LacI in a thermodynamic framework. First, Record and colleagues monitored *in vivo* repression as a function of intracellular potassium concentration [14]. Surprisingly, even though *in vitro* DNA binding shows a strong dependence on salt concentration, repression was not sensitive to such changes, [15,16]. Thus, perturbations that alter K_d *in vitro* do not necessarily translate into a predictable change *in vivo*. Consequently, to interpret *in vivo* results from an ongoing study of ~800 LacI/GalR variants, the relationship between ΔK_d and Δrepression must be determined for mutational perturbation. Second, Lewis and colleagues recently used thermodynamic analyses to describe the *in vivo* allosteric response for variants of LacI, but no direct comparisons were made with *in vitro* data [17,18]. Thus, if *in vivo* function is impacted by other processes, such as concentration-dependence of inducer uptake or nonspecific DNA binding, that system component remains undetected. Again, meaningful interpretation of the *in vivo* data for the large LacI/GalR mutant data set requires comparisons with *in vitro* measurements to identify other processes that may contribute to repression.

2. The BirA transcription repressor

BirA is a member of the biotin protein ligase family that is found in nearly all organisms. In both eubacteria and archaebacteria, some members of this enzyme family also function as transcriptional repressors (Fig. 2, [19,20]). Evolution of bifunctionality presumably occurred *via* gene fusion of the coding sequences for the BirA enzyme and a DNA binding domain. Subsequently, the enzymatic and repressor functions became integrated, so that mechanistic details of the enzyme-catalyzed reaction support the repressor function and *vice versa*. The bifunctionality of BirA is key to regulating biotin homeostasis in bacteria.

A schematic of the *E. coli* Biotin Regulatory System illustrates the basic functions of the system (Fig. 2). BirA binds to the two small molecule substrates, biotin and ATP, and catalyzes synthesis of the activated form of biotin, bio-5′-AMP [21]. The enzyme: intermediate complex either interacts with the biotin carboxyl carrier protein subunit (BCCP) of the biotin-dependent carboxylase, acetyl CoA carboxylase (ACC), or forms a homo-dimer that binds specifically to the biotin operator sequence (bioO) of the biotin biosynthetic operon [19,22]. The hetero-dimeric interaction with BCCP leads to chemical

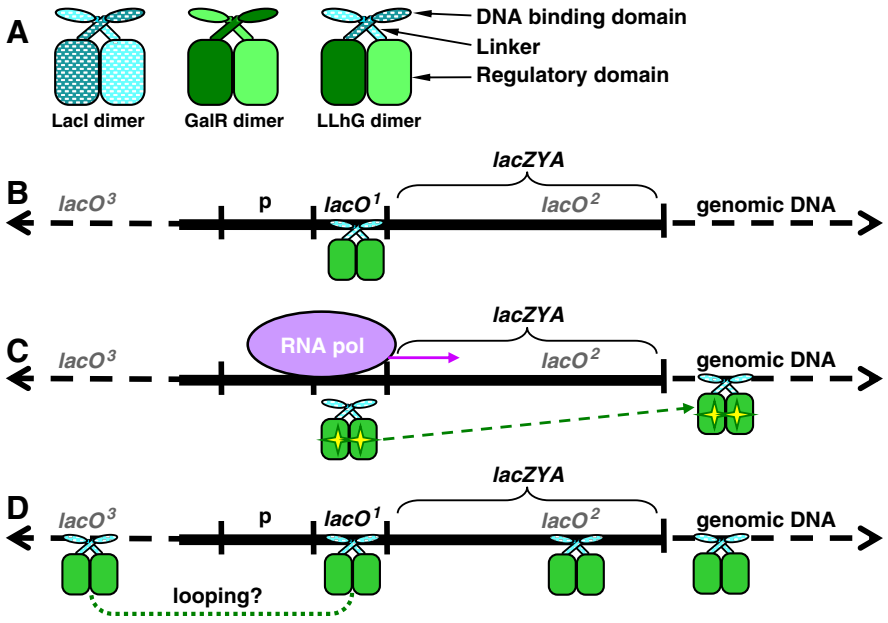

Fig. 1. Schematic of LacI/GalR homodimers and their binding to components of the *lac* operon. (A) The LacI homodimer is depicted as a stippled blue cartoon; the GalR homodimer is depicted in green; and the chimeric repressor LLhG is on the right. The small ovals depict the N-terminal DNA binding domains; bars depict the linker regions; and the large shapes depict the regulatory domains. (B) When a repressor binds to the $lacO^1$ operator sequence, transcription of the downstream *lacZYA* genes is repressed. (C) When inducer ligand (yellow stars) binds to repressor protein, affinity for $lacO^1$ is diminished. This allows polymerase to transcribe *lacZYA*, and the repressor-inducer complex binds to genomic DNA. (D) Other regions of the *E. coli* genome compete for binding repressor protein, including $lacO^2$, $lacO^3$, and genomic DNA. Wild-type GalR can form protein–protein interactions *via* the regulatory domains of two dimers [36]; thus, the potential exists for LLhG to do similarly.

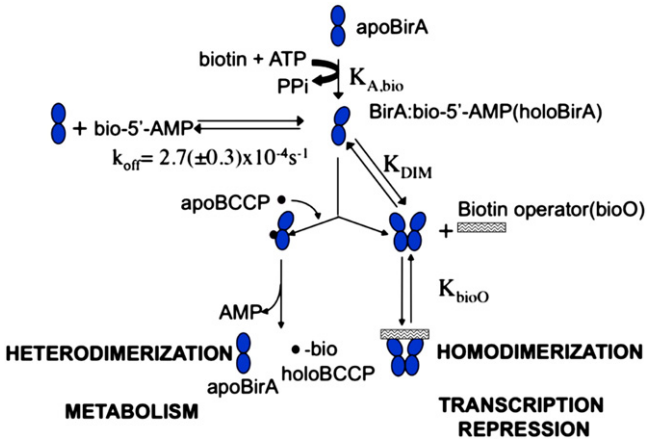

Fig. 2. Schematic outline of the *Escherichia coli* Biotin Regulatory System. See text for details.

transfer of biotin to a unique lysine residue on BCCP, where it is utilized for malonyl CoA biosynthesis. The homo-dimeric interaction leads to repression of transcription initiation at the biotin biosynthetic operon. Partitioning of the holoBirA complex between its two functions is regulated by the physiological demand for biotin [23]. Under conditions of rapid growth, biotinylation of ACC is in high demand because malonyl CoA biosynthesis constitutes the first committed step of fatty acid biosynthesis. Rapid growth rate, therefore, favors partitioning of holoBirA toward its enzymatic function. Once growth slows, the demand for biotin decreases and holoBirA partitions toward its transcription repression function, with the ultimate outcome of decreased biotin biosynthesis.

At a molecular level, it is the protein partner with which the enzyme-intermediate forms a dimer that determines BirA function [24,25]. In quantitative modeling of transcription repression, the interactions that contribute to holoBirA occupancy of the biotin operator include: substrate biotin binding, holoBirA homo-dimerization, and apoBCCP hetero-dimerization with holoBirA. In this work, the validity of this model has been tested by measuring the biotin concentration dependence of *bioO* occupancy *in vitro* and *in vivo*.

3. Materials and methods

3.1. LLhG methods

For this work, variants of LLhG/E62K/E230K were chosen because they exhibit stronger repression than LLhG/E320K [9]. The higher affinity of the E62K mutant for DNA renders the equilibrium binding affinity within the limits of measurements using the filter binding assay. As in previous publications, all references in the manuscript to LLhG include the implicit "E230K" designation. For simplicity, the E62K mutation is referred to as "+K".

LLhG + K variants were constitutively expressed from the plasmid pHG165a [9] and grown in BLIM cells [26] in 2xYT media overnight at 37 °C with shaking. The cell pellet was resuspended in 100 mL of cold breaking buffer (12 mM Hepes, 200 mM KCl, 1 mM EDTA, 5% glycerol, 0.3 mM DTT, pH to 8.0) with 1 protease inhibitor tablet (ROCHE Diagnostics, Indianapolis, IN, USA) and 50 mg of lysozyme. Cell paste was frozen at −20 °C, then thawed on ice with an additional 300 mL cold breaking buffer. After cell lysis was complete, 160 μl of 20 mg/mL DNaseI was added along with $MgSO_4$ (final concentration ≤ 30 mM). Cell debris was removed by centrifugation at 7000 rpm for 50 min at 4 °C and the supernatant was subjected to a 37% ammonium sulfate precipitation. The precipitate was separated by centrifugation at 7000 rpm for 40 min at 4 °C. The pellet was resuspended in 70 mL of cold Buffer A (12 mM Hepes, 50 mM KCl, 1 mM EDTA, 5% glycerol, 0.3 mM DTT, pH to 8.0) and dialyzed against 1 L of Buffer A for 30 min at 4 °C. Dialysis was repeated with two additional buffer changes. The dialysate was cleared by centrifugation at 8000 rpm for 30 min at 4 °C. Supernatant was loaded onto a phosphocellulose column and washed with Buffer A. LLhG protein was eluted using a linear gradient of Buffer A and Buffer B (12 mM Hepes, 500 mM KCl, 1 mM EDTA, 5% glycerol, 0.3 mM DTT, pH to 8.0). Finally, the column was washed with Buffer B. Aliquots of purified protein were stored at −80 °C.

Purified LLhG + K requires high concentrations of DTT for activity (see below), and the A_{280} could not be used to determine protein concentration. Therefore, the concentration was estimated using the BioRad assay (BioRad, Inc., Hercules, CA), with bovine serum albumin (Fisher Biotech, Fair lawn, NJ, 07410) as a standard. The activity of each protein preparation was determined by stoichiometric assays [27] to be between 70 and 95%. Activities were used to correct K_d values determined from binding titrations. DNA binding affinities for LLhG + K and variants were measured by binding protein to ^{32}P-labeled *lacO*^{1} and separating the free and bound DNA through nitrocellulose filter paper, as for wild type LacI [28] and a different chimeric protein, LLhP [29]. The *lacO*^{1} binding sequence (5′-TTGTGAGCGGATAACAA-3′) comprised the central region of a 40 bp ds DNA oligomer [28] and was synthesized by Integrated DNA Technology (Coralville, IA). For affinity assays, the DNA concentration was fixed at least 10-fold below the value of K_d [27].

In initial trials, an unusual behavior for LLhG + K was observed. In the buffer used to characterize wild-type LacI and LLhP, when LLhG + K was bound to high affinity operators such as *lacO*^{1} or the symmetrized operator *lacO*^{sym} [30], the complex appeared to precipitate over time. This did not occur for low affinity complexes, such as LLhG + K/*lacO*^{1}/inducer fucose or LLhG + K bound to nonspecific DNA (not shown). A survey of solution conditions revealed that 3 mM DTT in a Tris buffer with lower pH (7.1) alleviated this problem. Therefore, prior to DNA binding assays, purified LLhG + K variants were dialyzed against buffer with 3 mM DTT. The first two 30 min dialyses were against HEPES/DTT buffer (12 mM Hepes, pH 7.53, 150 mM KCl, 0.1 mM EDTA buffer and 3 mM DTT) and the third buffer exchange was into Tris/DTT buffer (10 mM Tris, pH 7.13, 150 mM KCl, 0.1 mM EDTA, and 3 mM DTT). After mixing protein and DNA, a 30 min equilibration was required prior to filtration.

DNA binding affinities were determined in both the absence and presence of 10 mM inducer sugar fucose. Results were analyzed with nonlinear repression using the program GraphPad Prism 5 (GraphPad Software, Inc., La Jolla, CA) to determine values of K_d. The equation used in the analysis is provided in the Results and discussion section. Each determination of K_d reported in Table 1 is the average of at least three separate experiments from at least two different protein purifications. In the presence of inducer, binding affinities were weaker than can be accurately measured with the filter binding technique (the upper plateau of the binding curve cannot be reached).

Table 1
Affinities of LLhG variants for *lacO*^{1} and values for *in vivo* repression.

	K_d for *lacO*^{1} ($\times 10^{-10}$ M)[a]	Repression[b]
LLhG/E62K ("±K")	4.6 ± 0.5	0.22 ± 0.03
I48S ± K	40 ± 20	2.3 ± 0.3
V52A ± K	0.56 ± 0.02	0.02 ± 0.01
V52P ± K	15 ± 5	0.90 ± 0.10
V52S ± K	3 ± 1	0.08 ± 0.02
Q55I ± K	4 ± 2	0.77 ± 0.05
Q55V ± K	9 ± 2	2.7 ± 0.3
G58L ± K	≥80 ± 20	1.5 ± 0.2
G58K ± K	11 ± 4	0.35 ± 0.09
S61N ± K	7 ± 3	0.19 ± 0.05

[a] Values reported are the average of 3–5 independent determinations using at least two different protein preparations. Reported errors were determined from the standard deviation of the average.
[b] All values except that for Q55V + K are from Ref. [9].

However, assays +/− inducer were carried out in parallel using the same protein, the same dilution of ^{32}P-DNA, and the same filter. Thus, lower boundaries for values of K_d in the presence of inducer were estimated by fixing the upper plateau to the corresponding value in the absence of inducer.

Measurements of *in vivo* repression of *lacO*^{1} were previously reported for all LLhG variants [9] except Q55V + K. Repression was determined for this variant as published for the others.

3.2. BirA methods

The biotin repressor (BirA) protein was overexpressed from the plasmid pHBA (a gift from Anne Chapman-Smith) and purified from *E. coli* BL21(lDE3.) as described in Brown et al. [31] . The purified protein was >95% pure as judged by SDS-PAGE, and >90% active as determined using stoichiometric titrations with bio-5′-AMP monitored by fluorescence spectroscopy [32].

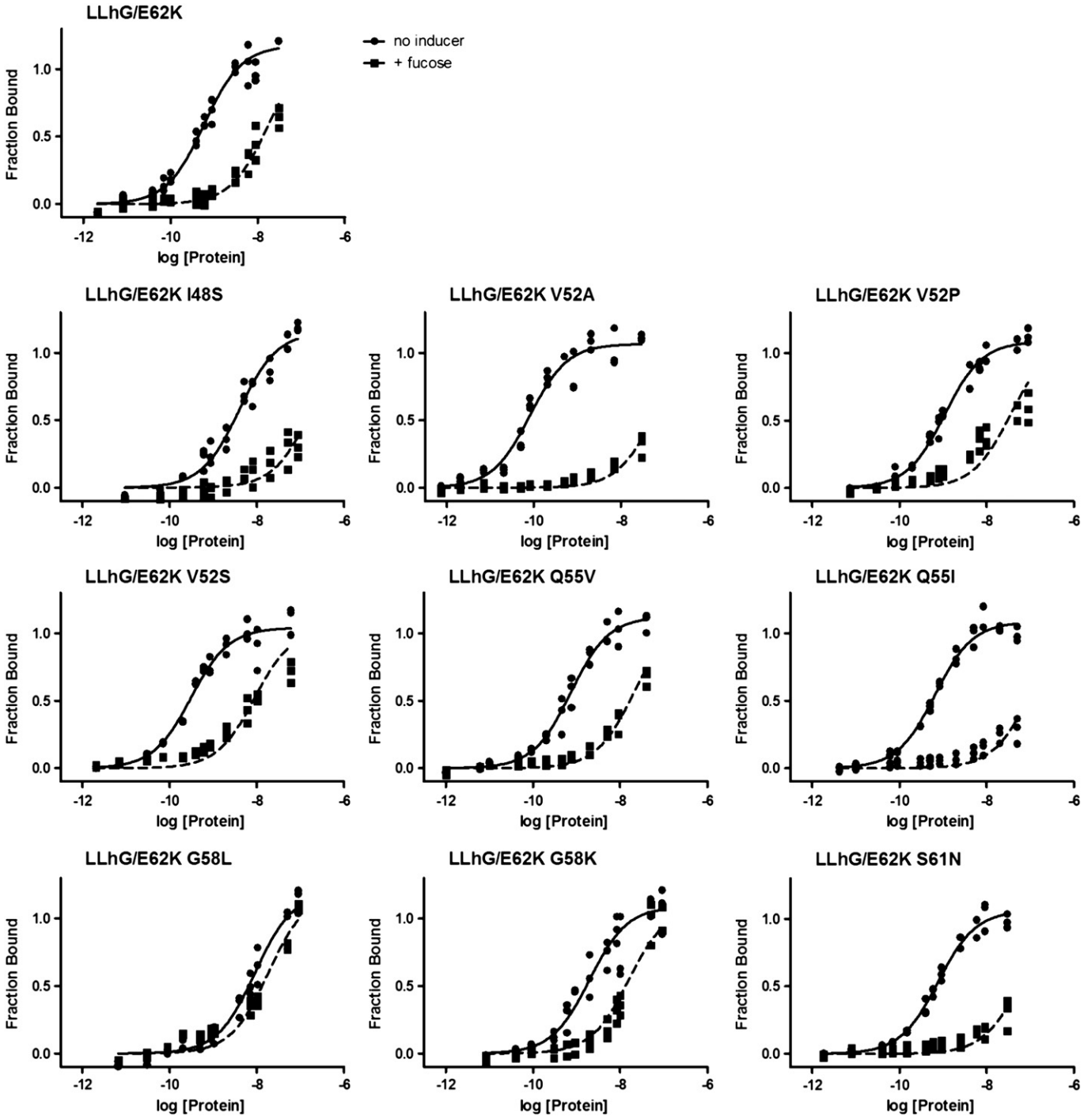

Fig. 3. Representative binding curves for LLhG variants. Binding to *lacO*^{1} was monitored in the absence (circles) and presence (squares) of inducer fucose. The solid line represents the best fit of Eq. 1 to the data measured in the absence of inducer; values of K_d were corrected for protein activity (see Methods); the average corrected values from three determinations are presented in Table 1. Since the −/+ inducer measurements were performed simultaneously – using the same DNA dilution, nitrocellulose filter, and exposure time – results from the fit in the absence of inducer were used to constrain fits of the data in the presence of inducer (dashed lines); these values range from $1–8\times10^{-8}$ M when corrected for protein activity.

The DNA fragment used in footprinting measurements was generated from restriction digestion of the plasmid pBioZ with *Hin*dIII, followed by labeling the purified, linearized DNA with α^{32}P dATP and dGTP using the Klenow fragment fill-in reaction [32]. Unincorporated nucleotides were removed from the labeled DNA by chromatography over an Elutip column (Millipore), and the DNA was subjected to phenol/chloroform extraction, ethanol precipitation, and digestion by *Pst* I. The final labeled fragment was separated from a second product by electrophoresis on a 1% agarose gel, recovered by electroelution, purified over an Elutip column and concentrated by ethanol precipitation. The radiolabeled DNA was stored at a final concentration of <20,000 cpm/μL (<8×10^{-3} pMol/μL) in TE buffer at 4 °C.

DNaseI footprinting measurements were performed using a variation of the method described in [32]. In these previous measurements, biotin operator occupancy was measured as a function of holoBirA concentration, and biotin and ATP were present in large excess to ensure saturation of BirA with bio-5′-AMP. In the present measurements, the *bioO* occupancy at a single BirA concentration was monitored as a function of biotin concentration. Thus, in all titrations, the *bioO* and ATP concentrations were held constant at ≤0.1 nM and 0.5 mM, respectively, and biotin concentration was varied. The BirA concentration in separate titrations was held constant at 7.5, 10 or 20 nM.

Binding reactions were performed in buffer containing 10 mM TrisHCl, pH 7.50 ± 0.02 at 37 °C, 200 mM KCl, 2.5 mM $MgCl_2$, 1 mM $CaCl_2$, 100 μg/mL BSA, and 20 μg/mL sonicated calf thymus DNA. Reaction mixtures were equilibrated at 37 °C for 1 h and DNaseI digestion was initiated by the addition of 5 μL of a freshly prepared DNaseI solution in wash buffer (Binding buffer-BSA, -Calf Thymus DNA). The DNaseI concentration in the final solution, approximately 15 ng/mL, was empirically set to ensure less than 50% digestion of the intact DNA [33]. After 2 min, the digestion was quenched by the addition of 33 μL of 50 mM Na_2EDTA, and the DNA was precipitated by the addition of 700 μL of 0.4 M NH_4OAc and 50 μg/mL tRNA in absolute ethanol. After centrifugation, the pellets were washed twice with 500 μL of cold 80% (v/v) absolute ethanol in water and dried by lyophilization. The dried pellets were dissolved in 7 μL of gel loading buffer containing 80% (v/v) deionized formamide, 1 × TBE, 0.02% (w/v) bromophenol blue, and 0.02% (w/v) xylene cyanol in water, heated for 10 min at 90 °C, and the digestion products were separated by electrophoresis on a 10% denaturing acrylamide gel. The gels were imaged using a Storm Phosphorimaging System (GE) and the resulting data were processed as described in Brenowitz et al. [33].

The biotin concentration-dependence of *in vivo* transcription from biotin biosynthetic operon promoter was determined using the *E. coli* strain CY481 (a gift from J.E. Cronan), which contains a fusion of the lacZ gene to the *bioB* promoter. Overnight cultures (10 mL) of the strain were grown at 37 °C with shaking in Minimal Media supplemented with biotin ranging in concentration from 0.8 nM to 0.1 μM. A 0.5 mL volume of each overnight culture was inoculated into 10 mL of fresh minimal media supplemented with the same biotin concentration. Cultures were grown with shaking at 37 °C until they reached mid-log phase ($O.D._{600\ nm} = 0.6$) at which point β-galactosidase assays were performed as described in [34].

Nonlinear least squares analysis of the titration data was performed using the program GraphPad Prism 4. The equation used in the analysis is provided in the Results and discussion section.

4. Results and discussion

4.1. LlhG: contributions of *lacO*^{1} binding affinity to repression of the lac operon

In previous studies, we determined *lacO*^{1} repression for LlhG/E62K ("LlhG + K") and >60 mutational variants [9]. From these, we chose 10 variants to purify and characterize *in vitro* (Table 1). Mutations are located at 5 different positions in the 18 amino acid linker that joins the LacI DNA binding domain to the GalR regulatory domain. Relative to LlhG + K, these variants exhibit a range of repression, both enhanced and diminished. The main goal of the current work was to ascertain whether the changes in repression correlate with altered *lacO*^{1} binding.

DNA binding assays were performed for each of the purified variants of LlhG + K. Data were analyzed with the equation:

$$Y_{obs} = \left(Y_{max} * \frac{[\mathrm{Prot}]}{K_d + [\mathrm{Prot}]}\right) + c \quad (1)$$

where "Y_{obs}" is the observed signal from ^{32}P-DNA, "Y_{max}" is the signal observed at saturation, "[Prot]" is the concentration of the LlhG + K variants, "c" is baseline value of the ^{32}P-DNA signal, and "K_d" is the equilibrium dissociation constant. Values determined for K_d in the absence of inducer are presented in Table 1 for the LlhG + K variants. No evidence of monomer-dimer dissociation was observed over the concentration range of the measurements (Fig. 3), which would manifest as slope >1 in the binding curve [35]. In the presence of inducer fucose, K_d decreased to between 1 and 8×10^{-8} M for the LlhG + L variants (Fig. 3).

As expected from repression values, some variants have higher affinity for *lacO*^{1} (lower value of K_d), whereas others have weaker affinity (larger value of K_d). Next, values of K_d were plotted against results from repression assays (Fig. 4). Across the dataset, both the repression and affinity data span ~2 orders of magnitude with an apparent linear correlation. Thus, changes in K_d translate into predictable changes for *in vivo* repression. However, results for two variants at position 55 (Q55I and Q55V) appear to have a trend that is distinct from the other repressors. Repression by the 55 variants is much weaker than would be anticipated from the DNA binding affinities, when compared to the other variants. This deviation can be highlighted with linear regression. When all 10 data points in Fig. 4 are included in linear regression, the best fit line (Fig. 4, black) has an R^2 value of 0.68; the line is more than one standard deviation away from the Q55 data points (error bars on black circles); and examination of the residuals shows that 2 points corresponding to the Q55 variants influence the distribution (Fig. 4, lower panel, filled *versus* open black circles). If the

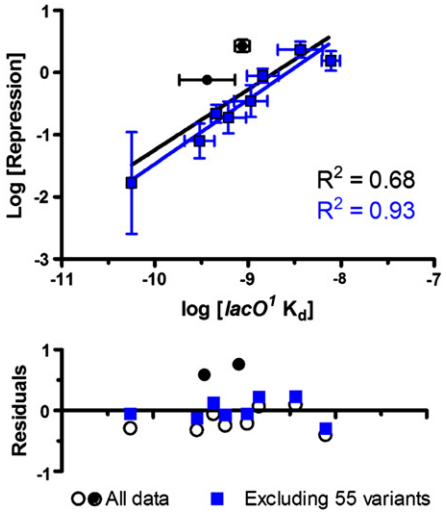

Fig. 4. Correlation of K_d and *in vivo* repression for LlhG variants. Values from Table 1 were plotted as log(repression) *versus* log(K_d) for all LlhG variants. If error bars are not visible, they are smaller than the size of the symbol. The upper, black line and R^2 value were determined by linear regression of all data. The lower, blue line and R^2 value were determined after excluding the values for LlhG/Q55V + K and LlhG/Q55I + K (black data points). A plot of the residuals is shown in the lower panel.

results for the Q55 variants are excluded, linear regression yields the blue line, which has an R^2 value of 0.93 and more evenly distributed residuals (Fig. 4, lower panel, blue squares).

Why is transcription repression by the Q55 variants weaker than predicted from *lacO*^{1} DNA binding affinities? The discrepancy is unlikely to be due to *in vivo* solution conditions, which should affect all of the variants equally. Instead, it may be due to changes in other equilibria that contribute to *in vivo* repression. As noted in the introduction, candidate interactions include looping with the *lacO*^{2} and *lacO*^{3} operators and competition from nonspecific genomic DNA. The parent protein of LLhG (GalR) can loop two operators *via* association of regulatory domains from two dimers [36]; LLhG + K variants might be able to do the same. Neither looping nor tetramerization is detected in the current *in vitro* assay, because the 40 basepair DNA oligomer only contains a single *lacO*^{1} binding site. If looping is involved in LLhG + K repression, then the decreased repression of the Q55 variants could result from decreased affinity for *lacO*^{2} or *lacO*^{3} relative to the remaining variants. If competition with nonspecific genomic DNA is involved, then the 55 variants must have enhanced nonspecific binding relative to the remaining variants.

Both 55 variants have the same direction of the deviation, compared to the other 8 variants of LLhG + K. However, both of the substituted amino acids (I and V) are smaller than Q and have a branched C^{β}. Thus, these two variants may have changed/lost the same interaction(s) that give rise to the diminished repression. This possibility is in agreement with information from available structures of two homologs, which show that the Q in wild-type LacI makes more contacts with the regulatory domain than the S that is present at this position in wild-type PurR [37].

The behaviors of the 55 variants underscore the complementary nature of *in vivo* and *in vitro* functional experiments. In addition to being amenable to large numbers of protein variants, *in vivo* assays are sensitive to unexpected functional changes. *In vitro* assays are required to understand which particular parameters are altered by mutation. An iterative comparison of the two approaches is required for a full description of functional change.

4.2. Reconciling *in vitro* LLhG + K binding curves with *in vivo* protein concentrations

The current data also allow correlation between the *in vitro* binding curves and estimated *in vivo* repressor concentrations. To that end, the number of repressor protein dimers per cell was estimated using immobilized DNA to capture the repressor from crude cell extracts (DNA pull-down assay) [9]; for LLhG + K, the estimate is ≥2500 copies per cell. This value is a low estimate, because (1) the calculation uses the lower limit of Coomassie stain for the protein concentration (50 ng) and (2) dilution shows that that the immobilized DNA is saturated with repressor. The volume of an *E. coli* cell is 0.44 to 1.79 um^3 (0.4 to 1.8 fL), depending on the culture media [38]. Repression assays are carried out in minimal media and thus should be on the low end of the range. Using these numbers, the estimated *in vivo* concentrations for both repressor and operator:

$$\left(2500 \text{ molecules repressor } / 6.023 \times 10^{23} \text{molecules / mole}\right) / \left(0.4 \times 10^{-15} \text{L}\right) = 1 \times 10^{-5} \text{M repressor per cell}$$

and

$$(1 \text{ operator / genome}) \times (\sim 2.3 \text{ genomes / cell}) / \left(6.023 \times 10^{23} \text{molecules / mole}\right) / \left(0.4 \times 10^{-15} \text{L}\right) = 9 \times 10^{-9} \text{M operator per cell.}$$

Based on the *in vitro* binding affinities, the *in vivo* protein concentrations fall in the saturation plateau for all of the curves (Fig. 5). However, the high repressor concentration does not agree with the estimated *in vivo* fractional occupancy of the operator, which was calculated from repression values (Table 1): A value of ~135 normalized Miller units corresponds to zero occupancy (no repressor present; data not shown) and assuming that a value of 0 Miller units corresponds to 100% occupancy (the lowest measured value is 0.017), the repression data for LLhG variants were rescaled. On this scale, operator occupancy is 98–99% for all LLhG + K variants, which occurs closer to 4×10^{-7} M protein (Fig. 5B). Even though this concentration is near the upper plateau of the binding curve, the occupancy differs for each value of K_d (Fig. 5B).

One possible explanation for the >25-fold discrepancy in protein concentration is that the *in vitro* and *in vivo* buffer conditions are sufficiently different to weaken K_d values by several orders of magnitude: Potential differences include *in vivo* crowding (reviewed in [39–41]) and ionic strength. Another compelling explanation is derived from considering linked equilibria: *In vivo,* operator and genomic nonspecific DNA are in competition for binding repressor.

The effects of *in vivo* crowding are difficult to predict. Crowding is expected to enhance the affinity of biomolecular associations except when one component is aspherical (such as genomic DNA) [39]. However, in a recent review of theoretical modeling, *in vitro* crowding agents, and *in vivo* measurements [41], Elcock noted that crowding appears to play a lesser role *in vivo* than predicted either *in vitro* or *in silico*. Likewise, changes in ionic strength do not have much effect on transcription repression by LacI [14]. Nonetheless, determining the best *in vitro* ionic strength remains an issue, because *in vitro* DNA binding is sensitive to that parameter [15,16]. The current experiments were performed in 150 mM KCl, which is in the range of

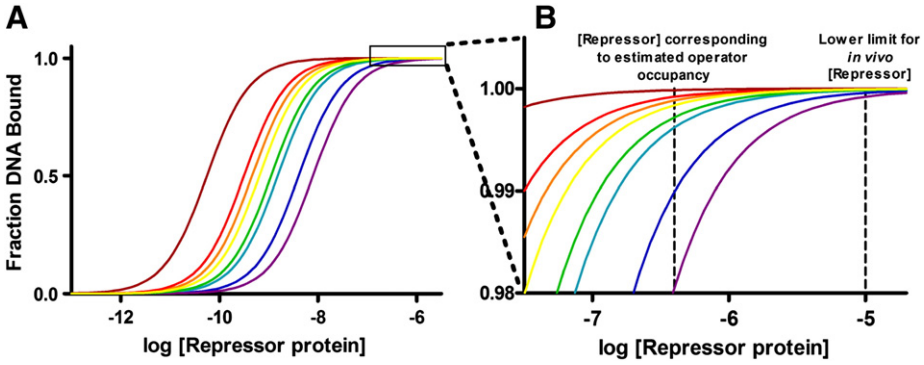

Fig. 5. LLhG binding curves, fractional *in vivo* occupancy, and estimated *in vivo* repressor concentration. (A) Ideal binding curves were calculated from the values in Table 1 for all LLhG + K variants except Q55V and Q55I. The boxed region is enlarged in panel (B), in order to show the estimated *in vivo* protein concentration (right dashed line) and the protein concentration that corresponds to fractional operator occupancy calculated from *in vivo* repression data (left dashed line; see text).

physiological potassium concentrations but probably lower in overall salt concentration than *in vivo* conditions, with the result being an over-estimate of DNA binding affinities.

Moreover, the processes of crowding, diffusion, and ionic strength may be inextricably connected to nonspecific DNA binding. Single molecule experiments indicate that, when not bound to the *lac* operator, LacI is bound to nonspecific DNA 90% of the time [13]. We expect similar behavior for other LacI/GalR proteins. Thus, the major macromolecule in the cellular vicinity of the repressor is genomic DNA, with its accompanying cloud of counter ions. Indeed, Record and co-workers proposed that nonspecific DNA binding buffered the effects of altered *in vivo* salt concentrations, so that repression by LacI was essentially not impacted [14]. The competition between *lacO* and nonspecific DNA has been considered extensively for wild-type LacI by the Riggs and von Hippel laboratories (*e.g.* [12,42–45]). For LacI, affinity for nonspecific DNA binding differs with DNA sequence and length. The tightest nonspecific interaction with poly[d(A+T)] has been estimated to be as high as 10^{-8} M [43] but the value probably approaches 3×10^{-4} M for "average" genomic DNA [12]. The effect of the competition on specific operator binding can be estimated using [12]:

$$K_{d,app} = K_{d,operator}\left(1 + Dt / K_{d,nonspecific}\right) \quad (2)$$

where $K_{d,app}$ is the apparent affinity constant for binding to the operator site, Dt is the total concentration of nonspecific DNA binding sites (~2×10^{-2} M; [42]), and $K_{d,nonspecific}$ is the affinity for non-specific DNA. Assuming that LLhG variants bind to nonspecific DNA with similar affinities to LacI, $K_{d,app}$ is ~70-fold weaker than $K_{d,operator}$, shifting the binding curves of Fig. 5 to the right. Remember that the estimated *in vivo* concentration for LLhG+K, and thus the 25-fold discrepancy, is a lower limit. Thus, the change in $K_{d,app}$ greatly reduces the discrepancy between *in vivo* repressor concentration and fractional operator occupancy.

4.3. BirA: modeling transcription repression

A shown in Fig. 2, assembly of holoBirA on the biotin operator sequence, *bioO*, is a two-step process in which homo-dimerization precedes operator binding [46]. Thus, the equilibrium expression for Fractional Saturation of *bioO* by holoBirA is:

$$\overline{Y} = \frac{K_{DIM}K_{bioO}[\text{holoBirA}]^2}{1 + K_{DIM}K_{bioO}[\text{holoBirA}]^2} \quad (3)$$

in which K_{DIM} and K_{bioO} are the equilibrium association constants governing holoBirA dimerization and binding of the dimer to *bioO*, respectively, and [holoBirA] is the concentration of the BirA·bio-5′-AMP complex. HoloBirA accumulation, which requires bio-5′-AMP synthesis, occurs by a mechanism in which biotin first binds followed by ATP [47]. Therefore, the Fractional Saturation of BirA with biotin dictates holoBirA concentration. Assuming the simplest model, in which biotin binding limits formation of the BirA·bio-5′-AMP complex, at any total BirA and biotin concentrations, holoBirA concentration is predicted using the following equation:

$$[\text{holoBirA}] = \overline{Y}_{BirA}[\text{BirA}]_{tot} = [\text{BirA}]_{tot}\frac{K_{A,biotin}[\text{biotin}]}{1 + K_{A,biotin}[\text{biotin}]} \quad (4)$$

in which $K_{A,biotin}$ is the equilibrium association constant for biotin binding to BirA and [biotin] is the free biotin concentration.

Combining Eqs. (3) and (4) allows prediction of the biotin-concentration dependence of *bioO* occupancy. In this work, a three-part comparison based on this model is made. First, the expected behavior was simulated using previously determined binding parameters. Second, *in vitro* binding of BirA to *bioO* was measured as a function of biotin concentration. Third, *in vivo* repression was determined as a function of exogenous biotin concentration.

The simulations utilized equilibrium parameters obtained from (i) ITC measurements of biotin binding to the BirA monomer [48], (ii) dimerization of holoBirA by sedimentation equilibrium [25,49], and (iii) *bioO* binding by DNaseI footprinting [50] to predict the biotin concentration dependence of *bioO* occupancy (Fractional Saturation) at three different total BirA concentrations (Fig. 6A). The range of BirA concentrations used for the simulations bracket the intracellular concentration of 2–200 nM estimated form quantitation of biotin binding activity in *E. coli* cell extracts [51]. Normalized transcription (Fig. 6B) was calculated as the quantity (1 - Fractional Saturation). All three Fractional Saturation and repression curves exhibit a steep dependence on biotin concentration that is attributable to the dependence of *bioO* occupancy on dimerization rather than any cooperativity in biotin binding (Fig. 6B). At the lowest BirA concentration of 2 nM, neither full occupancy nor full repression is achieved even at the highest biotin concentration.

4.4. BioO occupancy does not depend on biotin affinity alone

Next, the biotin-concentration dependence of BirA binding to *bioO* was directly determined using DNaseI footprinting experiments. The experimental conditions were based on the simulation, which showed that at 20 nM BirA and a saturating biotin concentration, saturation of *bioO* is achieved (Fig. 6, black curve). The footprinting experiments also included an ATP concentration sufficiently high to ensure complete conversion of BirA-bound biotin to bio-5′-AMP, the physiological effector. Surprisingly, comparison of the experimental binding isotherm to the simulated curve reveals a discrepancy of approximately 10-fold in the midpoint of the curves (Fig. 7). Since the simulation is based on known values of the relevant parameters, at

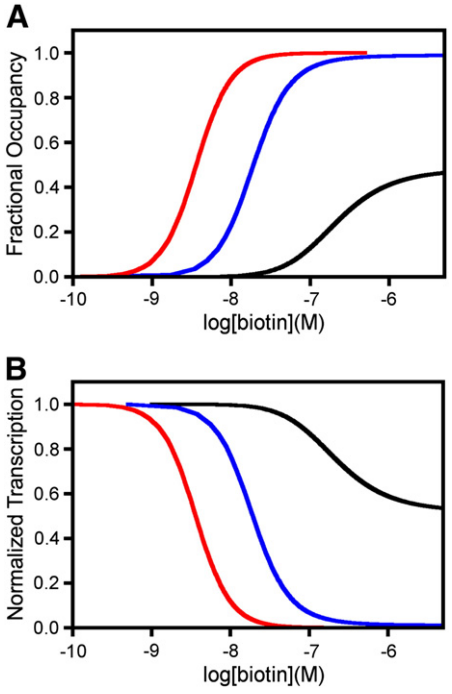

Fig. 6. Simulations of the [biotin] dependence of (A) *bioO* occupancy and (B) transcription repression at multiple BirA concentrations. Red (2×10^{-7} M), blue (2×10^{-8} M), black (2×10^{-9} M) BirA. Combined Eqs. 3 and 4 were used for the simulations with the values of $K_{DIM}K_{bioO}$ and $K_{A,biotin}$ set at 2.3×10^{17} M^{-3} [25] and 6.8×10^{6} M^{-1} [48], respectively.

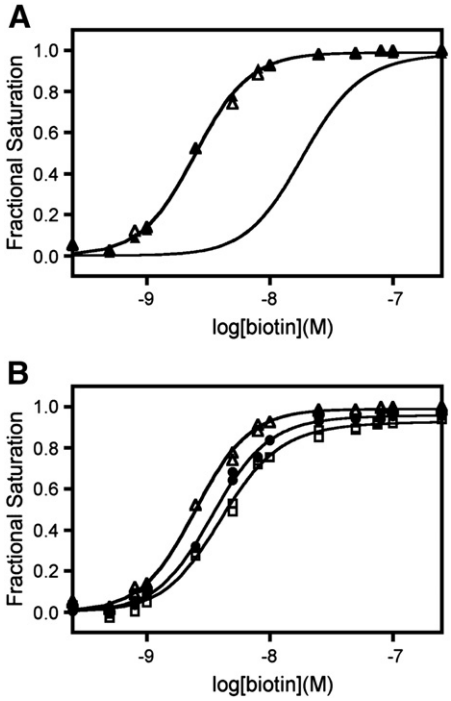

Fig. 7. (A) Simulation and measurement of the [biotin] dependence of Fractional Saturation of *bioO* by BirA. The triangles represent the Fractional Saturation of *bioO* by BirA determined using DNaseI footprinting. The solid curve on the right is dependence of occupancy on [biotin] simulated assuming that the affinity of BirA for biotin, alone, dictates [holoBirA] (Fig. 6). The solid line with the data points is the best-fit of the data to combined Eqs. 3 and 4. In the analysis the value of $K_{DIM}K_{bioO}$ was fixed at $2.3\times10^{17}\,M^{-3}$ and a value of $K_{A,biotin}$ of $2.7(\pm0.5)\times10^{8}\,M^{-1}$ was resolved. (B) Biotin concentration dependence of *bioO* occupancy measured at [BirA] of 20 (Δ), 10 (●) and 7.5 (□) nM. The lines represent the best-fit curves obtained from nonlinear least squares analysis of the data using Eqs. 3 and 4 to obtain values of $K_{A,biotin}$ of $1.7(\pm0.1)\times10^{8}\,M^{-1}$ and $1.6(\pm0.1)\times10^{8}\,M^{-1}$ at 10 and 7.5 nM BirA, respectively.

least one assumption of the model is likely to be incorrect. The parameter used for the product of the equilibrium dimerization constant and the equilibrium constant governing the dimer binding to *bioO* was experimentally determined [25]. Likewise, the equilibrium constant governing biotin binding to BirA was also experimentally determined [48]. Thus, the assumption that holoBirA concentration is governed by biotin binding alone must be incorrect.

Further consideration of the model in Fig. 2 serves as a reminder that biotin binding to BirA is coupled to ATP binding, with resulting bio-5′-AMP synthesis and allosteric activation of repressor dimerization [47,49,52] (Fig. 2). Substrate binding is obligatorily ordered, with biotin binding first followed by ATP. Binding of the adenylate to the BirA monomer is very tight and is characterized by an equilibrium association constant of $2.5\times10^{10}\,M^{-1}$ at 20 °C, a value 1000-fold larger than the association constant governing biotin binding, which is $6.8\times10^{6}\,M^{-1}$ [47,48]. However, when the binding isotherm at 20 nM BirA was analyzed with the combined Eqs. 3–4, with the product of the dimerization and DNA binding constants ($K_{DIM}K_{bioO}$) fixed at the experimentally determined value of $2.3\times10^{17}\,M^{-3}$[25], an apparent equilibrium association constant for biotin binding yielded a value of $2.7(\pm0.5)\times10^{8}\,M^{-1}$ (Fig. 7A), ~40-fold tighter than measured for biotin binding to apo-BirA. To determine the consistency of this parameter, footprint titrations were repeated using BirA concentrations of 7.5 and 10 nM; results yield apparent equilibrium constants for biotin binding of the same magnitude (Fig. 7B). A reasonable explanation of the discrepancy between equilibrium constant for biotin binding alone and this "effective" equilibrium constant lies in the coupling of biotin and ATP binding, which results in an equilibrium association constant that is 30–40-fold larger than that for biotin alone.

4.5. In vivo biotin-concentration dependent transcription repression shows good agreement with in vitro binding

Finally, the *in vivo* dependence of transcription repression by BirA was determined as a function of exogenous biotin concentration. Transcription repression at the biotin operon promoter, P_A, was measured using a strain in which the *lacZ* gene was fused to the *bioF* gene [53]. Disruption of the *bioF* gene by fusion to *lacZ* renders the strain auxotrophic for biotin and intracellular biotin concentrations are regulated by the concentration provided in the media. Multiple independent measurements of the β-galactosidase activity yielded maximal values at the lowest biotin concentration ranging from 180 to 200 Miller units. At the highest biotin concentrations, the activity in Miller units was approximately 1. Plots of the normalized repression as a function of biotin concentration (Fig. 8, open circles) show the same steep dependence on biotin concentration that is predicted by the model (Fig. 6). However, the repression curve is shifted to higher biotin concentrations than observed in the repression curve generated from the *in vitro* footprinting measurements of the biotin concentration-dependence of *bioO* occupancy (Fig. 7 and transformed in Fig. 8, triangles).

The discrepancy between the *in vitro* and *in vivo* titrations could reflect several possible contributing factors, including differences between *in vivo* and *in vitro* solution conditions and uncertainties in *in vivo* protein concentrations. Unlike the LacI/GalR proteins, nonspecific DNA binding is not observed even at the relatively low KCl concentration of 50 mM and thus is not a factor in BirA repression [50].

To reconcile repression with binding affinities determined by DNaseI footprinting, *in vivo* "solution" conditions must weaken K_a values compared to those determined *in vitro*. To estimate the magnitude of the difference, nonlinear least squares analysis of the repression data was carried out using combined Eqs. (3) and (4) to obtain the product of the equilibrium association constants governing dimerization and dimer binding to *bioO*, $K_{DIM}\ K_{bioO}$. In this analysis, the equilibrium association constant for biotin was fixed at the value of $2\times10^{8}\,M^{-1}$ that was obtained from the DNaseI footprint titrations describe above. The best-fit value of $K_{DIM}\ K_{bioO}$, $2.4(\pm0.4)\times10^{16}\,M^{-3}$, differs 10-fold from that obtained from the *in vitro* DNAseI footprinting titrations ($2.3\times10^{17}\,M^{-3}$) [25].

Another potential source of the discrepancy in analysis of the *in vivo* repression data is *in vivo* protein concentration. In the present analysis, the total BirA concentration was fixed at 20 nM, a value that is estimated from measurement of the biotin binding activity present in *E. coli* extracts [51]. This value must be experimentally determined for cultures in parallel with transcription measurements. A lower *in vivo* BirA concentration would yield a value more in line with the results of footprint titrations. A second uncertainty is the *in vivo* BCCP

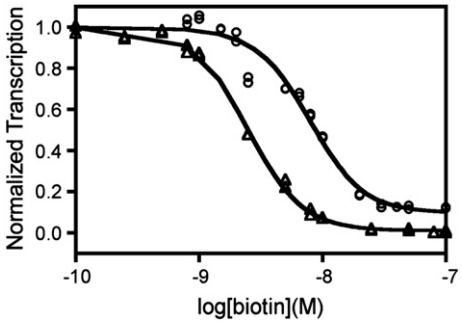

Fig. 8. *In vitro* and *in vivo* measurements of the [biotin] dependence of *bioO* occupancy (transcription). Triangles represent the normalized transcription predicted from the measured [biotin] concentration dependence of *bioO* occupancy (Fig. 7). The circles (duplicate measurements at each biotin concentration) represent the normalized transcription measured as a function of [biotin] concentration. In each case the line represents the best-fit of the data to combined Eqs. 3 and 4 (see text).

concentration, which would effectively decrease the steady-state holoBirA concentration by its conversion to apoBirA *via* catalysis (Fig. 2). This latter factor is particularly significant for measurements performed on rapidly dividing cultures, such as those used in these measurements, due to the positive correlation of BCCP (and the remaining three subunits of acetyl CoA carboxylase) synthesis with growth rate [54].

5. Conclusion

To unite *in vitro* and *in vivo* analyses of protein function, two types of information are commonly assumed to be necessary (i) a full description of all linked equilibria that participate in the biological function; and (ii) knowledge of which *in vitro* solution conditions best match cellular conditions. Several decades of work have been devoted to mimicking cellular conditions in the test tube, using additives such as Ficoll (reviewed in [39]). In the past decade, new studies have directly quantitated *in vivo* protein folding/stability to compared results with *in vitro* measurements [55,56]. Surprisingly, the results suggest that the effects of cellular "solution" conditions, especially crowding, do not necessarily dominate protein folding behaviors *in vivo* [41].

This feature might be extendable to protein function: In the current study, the *in vitro* functions for two different repressor proteins – in two different assay buffers and subject to two different mechanisms to vary K_d – both show strong correlations with *in vivo* functional data. Equilibria appear to be shifted left or right, but the protein behavior is not fundamentally altered. Note that both systems used changes other than solution conditions for altering K_d (mutation and ligand concentration, respectively).

The robust correlations for these two systems indicate that solution thermodynamic measurements are very useful for predicting changes in *in vivo* function. In turn, *in vivo* tests provide valuable information about strategies for improving the predictive capability of *in vitro* studies. For example, the addition of terms for coupled looping or nonspecific binding to the LacI/GalR model would help to improve the agreement between *in vitro* and *in vivo* results. A major challenge to bridging the divide between the model and the biological system is the accurate determination of intracellular protein concentrations, such as for BirA and BCCP. Potential solutions to this problem include Quantitative Western Blotting or *in vivo* labeling methods. Nevertheless, the reasonably close correlation between binding measurements and transcription repression found for the two systems illustrates the remarkable power of biothermodynamics to predict function in biological systems.

Acknowledgments

This work was supported by grants from the NIH and the ARRA stimulus funds to LSK (GM079423) and DB (GM46511). We thank Renae Springe and Josh Riepe for assistance purifying LLhG variants. We also thank Emily Streaker for preparation of the BirA that was used for these measurements.

References

[1] L. Swint-Kruse, K.S. Matthews, Allostery in the LacI/GalR family: variations on a theme, Curr. Opin. Microbiol. 12 (2009) 129–137.
[2] M.J. Weickert, S. Adhya, A family of bacterial regulators homologous to Gal and Lac repressors, J. Biol. Chem. 267 (1992) 15869–15874.
[3] C.E. Bell, M. Lewis, A closer view of the conformation of the Lac repressor bound to operator, Nat. Struct. Biol. 7 (2000) 209–214.
[4] M.A. Schumacher, K.Y. Choi, H. Zalkin, R.G. Brennan, Crystal structure of LacI member, PurR, bound to DNA: minor groove binding by alpha helices, Science 266 (1994) 763–770.
[5] A. Majumdar, S. Adhya, Demonstration of two operator elements in gal: in vitro repressor binding studies, Proc. Natl. Acad. Sci. U. S. A. 81 (1984) 6100–6104.
[6] M.A. Schumacher, G.S. Allen, M. Diel, G. Seidel, W. Hillen, R.G. Brennan, Structural basis for allosteric control of the transcription regulator CcpA by the phosphoprotein HPr-Ser46-P, Cell 118 (2004) 731–741.
[7] S. Alberti, S. Oehler, B. von Wilcken-Bergmann, H. Krämer, B. Müller-Hill, Dimer-to-tetramer assembly of *lac* repressor involves a leucine heptad repeat, New Biol. 3 (1991) 57–62.
[8] K.S. Matthews, DNA Looping, Microbiol. Rev. 56 (1992) 123–136.
[9] S. Meinhardt, L. Swint-Kruse, Experimental identification of specificity determinants in the domain linker of a LacI/GalR protein: bioinformatics-based predictions generate true positives and false negatives, Proteins 73 (2008) 941–957.
[10] M.C. Mossing, M.T. Record Jr., Upstream operators enhance repression of the lac promoter, Science 233 (1986) 889–892.
[11] S. Oehler, E.R. Eismann, H. Kramer, B. Müller-Hill, The three operators of the lac operon cooperate in repression, EMBO J. 9 (1990) 973–979.
[12] S. Lin, A.D. Riggs, The general affinity of lac repressor for E. coli DNA: implications for gene regulation in procaryotes and eucaryotes, Cell 4 (1975) 107–111.
[13] J. Elf, G.W. Li, X.S. Xie, Probing transcription factor dynamics at the single-molecule level in a living cell, Science 316 (2007) 1191–1194.
[14] B. Richey, D.S. Cayley, M.C. Mossing, C. Kolka, C.F. Anderson, T.C. Farrar, M.T. Record, Variability of the intracellular ionic environment of Escherichia coli. Differences between in vitro and in vivo effects of ion concentrations on protein-DNA interactions and gene expression, J. Biol. Chem. 262 (1987) 7157–7164.
[15] M.C. Mossing, M.T. Record Jr., Thermodynamic origins of specificity in the lac repressor-operator interaction. Adaptability in the recognition of mutant operator sites, J. Mol. Biol. 186 (1985) 295–305.
[16] P.A. Whitson, J.S. Olson, K.S. Matthews, Thermodynamic analysis of the lactose repressor-operator DNA interaction, Biochemistry 25 (1986) 3852–3858.
[17] R. Daber, K. Sharp, M. Lewis, One is Not Enough, J. Mol. Biol. 392 (2009) 1133–1144.
[18] R. Daber, M.A. Sochor, M. Lewis, Thermodynamic Analysis of Mutant lac Repressors, J. Mol. Biol. 409 (2011) 76–87.
[19] D.F. Barker, A.M. Campbell, Genetic and biochemical characterization of the birA gene and its product: evidence for a direct role of biotin holoenzyme synthetase in repression of the biotin operon in *Escherichia coli*, J. Mol. Biol. 146 (1981) 469–492.
[20] D.A. Rodionov, A.A. Mironov, M.S. Gelfand, Conservation of the biotin regulon and the BirA regulatory signal in Eubacteria and Archaea, Genome Res. 12 (2002) 1507–1516.
[21] M.D. Lane, K.L. Rominger, D.L. Young, F. Lynen, The enzymatic synthesis of holotranscarboxylase from apotranscarboxylase and (+)-biotin. II. Investigation of the reaction mechanism, J. Biol. Chem. 239 (1964) 2865–2871.
[22] O. Prakash, M.A. Eisenberg, Biotinyl 5′-adenylate: corepressor role n the regulation of the biotin genes of *Escherichia coli* K-12, Proc. Natl. Acad. Sci. U. S. A. 76 (1979) 5592–5595.
[23] J.E. Cronan Jr., Expression of the biotin biosynthetic operon of *Escherichia coli* is regulated by the rate of protein biotination, J. Biol. Chem. 263 (1988) 10332–10336.
[24] E.D. Streaker, D. Beckett, The biotin regulatory system: kinetic control of a transcriptional switch, Biochemistry 45 (2006) 6417–6425.
[25] H. Zhao, D. Beckett, Kinetic partitioning between alternative protein–protein interactions controls a transcriptional switch, J. Mol. Biol. 380 (2008) 223–236.
[26] D.R. Wycuff, K.S. Matthews, Generation of an Ara-C-*ara*BAD promoter-regulated T7 expression system, Anal. Biochem. 277 (2000) 67–73.
[27] L. Swint-Kruse, K.S. Matthews, Thermodynamics, protein modification, and molecular dynamics in characterizing lactose repressor protein: strategies for complex analyses of protein structure-function, Methods Enzymol. 379 (2004) 188–209.
[28] H. Zhan, L. Swint-Kruse, K.S. Matthews, Extrinsic interactions dominate helical propensity in coupled binding and folding of the lactose repressor protein hinge helix, Biochemistry 45 (2006) 5896–5906.
[29] H. Zhan, M. Taraban, J. Trewhella, L. Swint-Kruse, Subdividing repressor function: DNA binding affinity, selectivity, and allostery can be altered by amino acid substitution of nonconserved residues in a LacI/GalR homologue, Biochemistry 47 (2008) 8058–8069.
[30] J.R. Sadler, H. Sasmor, J.L. Betz, A perfectly symmetric lac operator binds the lac repressor very tightly, Proc. Natl. Acad. Sci. U. S. A. 80 (1983) 6785–6789.
[31] P.H. Brown, J.E. Cronan, M. Grotli, D. Beckett, The biotin repressor: modulation of allostery by corepressor analogs, J. Mol. Biol. 337 (2004) 857–869.
[32] J. Abbott, D. Beckett, Cooperative binding of the *Escherichia coli* repressor of biotin biosynthesis to the biotin operator sequence, Biochemistry 32 (1993) 9649–9656.
[33] M. Brenowitz, D.F. Senear, M.A. Shea, G.K. Ackers, Quantitative DNase footprint titration: a method for studying protein-DNA interactions, Methods Enzymol. 130 (1986) 132–181.
[34] J.H. Miller, Experiments in Molecular Genetics, Cold Spring Harbor Laboratory, Cold Spring Harbor, NY, 1972.
[35] J. Chen, K.S. Matthews, Subunit dissociation affects DNA binding in a dimeric lac repressor produced by C-terminal deletion, Biochemistry 33 (1994) 8728–8735.
[36] S. Semsey, K. Virnik, S. Adhya, Three-stage regulation of the amphibolic gal operon: from repressosome to GalR-free DNA, J. Mol. Biol. 358 (2006) 355–363.
[37] L. Swint-Kruse, C. Larson, B.M. Pettitt, K.S. Matthews, Fine-tuning function: correlation of hinge domain interactions with functional distinctions between LacI and PurR, Protein Sci. 11 (2002) 778–794.
[38] H.E. Kubitschek, J.A. Friske, Determination of bacterial cell volume with the Coulter Counter, J. Bacteriol. 168 (1986) 1466–1467.
[39] H.X. Zhou, G. Rivas, A.P. Minton, Macromolecular crowding and confinement: biochemical, biophysical, and potential physiological consequences, Annu. Rev. Biophys. 37 (2008) 375–397.
[40] G.J. Pielak, A.C. Miklos, Crowding and function reunite, Proc. Natl Acad. Sci. 107 (2010) 17457–17458.

[41] A.H. Elcock, Models of macromolecular crowding effects and the need for quantitative comparisons with experiment, Curr. Opin. Struct. Biol. 20 (2010) 196–206.
[42] P.H. von Hippel, A. Revzin, C.A. Gross, A.C. Wang, Non-specific DNA binding of genome regulating proteins as a biological control mechanism: 1. The lac operon: equilibrium aspects, Proc. Natl Acad. Sci. 71 (12) (1974) 4808–4812.
[43] S.Y. Lin, A.D. Riggs, Lac repressor binding to non-operator DNA: detailed studies and a comparison of equilibrium and rate competition methods, J. Mol. Biol. 72 (1972) 671–690.
[44] Y. Kao-Huang, A. Revzin, A.P. Butler, P. O'Conner, D.W. Noble, P.H. von Hippel, Nonspecific DNA binding of genome-regulating proteins as a biological control mechanism: measurement of DNA-bound *Escherichia coli* lac repressor in vivo, Proc. Natl. Acad. Sci. U. S. A. 74 (1977) 4228–4232.
[45] P.H. von Hippel, A. Revzin, C.A. Gross, A.C. Wang, Interaction of lac repressor with non specific DNA binding sites, Protein Ligand Interact. Symp. (1974) 270–280.
[46] E.D. Streaker, D. Beckett, Coupling of protein assembly and DNA binding: biotin repressor dimerization precedes biotin operator binding, J. Mol. Biol. 325 (2003) 937–948.
[47] Y. Xu, D. Beckett, Kinetics of biotinyl-5′-adenylate synthesis catalyzed by the *Escherichia coli* repressor of biotin biosynthesis and the stability of the enzyme-product complex, Biochemistry 33 (1994) 7354–7360.
[48] Y. Xu, C.R. Johnson, D. Beckett, Thermodynamic analysis of small ligand binding to the *Escherichia coli* repressor of biotin biosynthesis, Biochemistry 35 (1996) 5509–5517.
[49] E. Eisenstein, D. Beckett, Dimerization of the *Escherichia coli* biotin repressor: corepressor function in protein assembly, Biochemistry 38 (1999) 13077–13084.
[50] H. Zhao, E. Streaker, W. Pan, D. Beckett, Protein–protein interactions dominate the assembly thermodynamics of a transcription repression complex, Biochemistry 46 (2007) 13667–13676.
[51] M.A. Eisenberg, O. Prakash, S.C. Hsiung, Purification and properties of the biotin repressor. A bifunctional protein, J. Biol. Chem. 257 (1982) 15167–15173.
[52] E.D. Streaker, A. Gupta, D. Beckett, The biotin repressor: thermodynamic coupling of corepressor binding, protein assembly, and sequence-specific DNA binding, Biochemistry 41 (2002) 14263–14271.
[53] D.F. Barker, A.M. Campbell, Use of bio-lac fusion strains to study regulation of biotin biosynthesis in *Escherichia coli*, J. Bacteriol. 143 (1980) 789–800.
[54] S.J. Li, J.E. Cronan Jr., Growth rate regulation of *Escherichia coli* acetyl coenzyme A carboxylase, which catalyzes the first committed step of lipid biosynthesis, J. Bacteriol. 175 (1993) 332–340.
[55] A. Gershenson, L.M. Gierasch, Protein folding in the cell: challenges and progress, Curr. Opin. Struct. Biol. 21 (2011) 32–41.
[56] S. Ghaemmaghami, T.G. Oas, Quantitative protein stability measurement in vivo, Nat. Struct. Biol. 8 (2001) 879–882.